Journal Name

ARTICLE

A novel magnetic nano particles with ionic liquids tags as a reusable catalyst in the synthesis of polyhydroquinolines

Received 00th January 20xx,
Accepted 00th January 20xx

DOI: 10.1039/x0xx00000x

www.rsc.org/

Meysam Yarie[a], Mohammad Ali Zolfigol*[a], Yadollah Bayat[b], Asiye Asgari[b], Diego A. Alonso*[c], and Abbas Khoshnood*[c]

In this paper, we have introduced {Fe_3O_4@SiO_2@$(CH_2)_3$Im}$C(NO_2)_3$ as a novel and heterogeneous reusable catalyst for the four component preparation of the polyhydroquinoline derivatives under mild and eco-friendly reaction conditions. The structural confirmation of the novel heterogeneous reusable promoter was fully made using appropriate technical skills such as FT-IR, X-ray diffraction patterns (XRD), Field emission scanning electron microscopy (FESEM), Energy-dispersive spectroscopy (EDS) elemental mapping analysis, High Resolution transmission electron microscopy (HRTEM), thermogravimetry (TG), derivative thermal gravimetric (DTG), differential thermal (DTA) and vibrating sample magnetometer (VSM) analysis. The presented nano magnetic heterogeneous catalyst was successfully applied for the synthesis of the polyhydroquinoline derivatives *via* a four component condensation of a good range arylaldehydes, dimedone, ethyl acetoacetate or methyl acetoacetate as *β*-ketoester, and ammonium acetate as nitrogen source under solvent free conditions. Also, the experimental evidence has demonstrated that the {Fe_3O_4@SiO_2@$(CH_2)_3$Im}$C(NO_2)_3$ could act as a nano magnetically recoverable and reusable catalyst without any meaningful drop in the yield and the reaction time at least for eight times.

Keywords: Magnetic nano particles, {Fe_3O_4@SiO_2@$(CH_2)_3$Im}$C(NO_2)_3$, heterogeneous reusable catalyst, trinitromethane, nitroform, polyhydroquinoline, solvent free conditions

Introduction

In recent times, development and expanding of the magnetic nano particles (MNPs) as versatile supports be revealed as an influential branch in the field of green chemistry due to the environmentally benign nature of these compounds. For the reason of easy separation of the magnetically based materials from the reaction system, many attempts were focused for the surface modification of them in order to construct varied heterogeneous magnetically recoverable promoters for the organic functional transformation [1]. Also, using nano magnetic heterogeneous catalytic systems for promotion of the reaction, represent high catalytic performance as in the case of the homogeneous catalysts and passed them from the facile and efficient recovery point of view through applying a simple external magnet and these merits led to a surprising spread of their potential applicability's [2]. The chemistry of MNPs have been extensively reviewed [1-3].

On the other hand, the capabilities of the ionic liquids as reagents, catalyst, reaction media and proper solvent for different goals in the field of green chemistry are well documented in past few years [4-10]. Although the widespread applications of ionic liquids, investigations have disclosed that in some case the ionic liquids disadvantaged due to the toxic nature of them [11,12]. Therefore, it is worthy that the ongoing studies impact on the enhancement of the defects connected with conventional not safe ionic liquids and replacing them with safer and more productive ones. Therefore, the combination of the ionic liquids and magnetic nano particles (MNPs) as versatile supports for the immobilization of the ionic liquids offers several merits such as easy synthesis pathway, large surface area, high thermal stability, facile separation from the reaction mixture, and low toxicity and price [13].

The building up of the complex compounds with high atom and step economy, improvement of the effectiveness and plainness in the synthetic pathway, providing easy and straightforward approach to library molecules and diversity-oriented synthesis (DOS) are the principal interest of the one pot multicomponent reactions (MCRs) and this beneficial technical protocol persuaded both academic and industrial chemists to access molecular diversity by this way [14-17].

Recently, due to the varied pharmaceutical and biological applications connected to the polyhydroquinolines structural motif, a huge attention has been paid to the production of these versatile organic compounds. Substituted 1,4-dihydropyridines are renowned as calcium channel modulators and they can be applied as a treatment for the therapy of the cardiovascular diseases [18].

[a] Department of Organic Chemistry, Faculty of Chemistry, Bu-Ali Sina University, Hamedan, Iran. Fax: +988138257407, E-mail: zolfi@basu.ac.ir;
[b] Faculty of Chemistry and chemical Engineering, Malek Ashtar University of Technology, Tehran, Iran
[c] Organic Chemistry Department and Organic Synthesis Institute, Alicante University, Apdo. 99, 03080 Alicante, Spain. Phone: +34965909841, E-Mail: diego.alonso@ua.es; abbas.khoshnood@ua.es

Some biologically active species base on 1,4-dihydropyridines moiety are illustrated in Fig. 1[19].

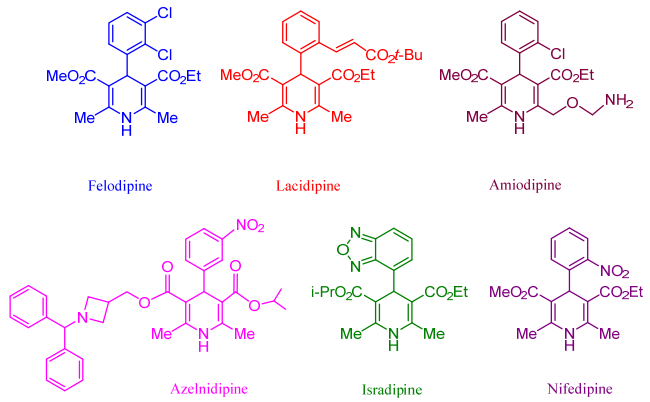

Fig. 1: Biologically active 1,4-dihydropyridines

Due to the above listed excellent therapeutic applications of the 1,4-dihydropyridine derivatives, synthetic chemists have explored several protocols for the synthesis of them using different reaction conditions and varied catalytic systems as follows: $Yb(OTf)_3$ [20], [pyridine-SO_3H]Cl [21], [Dsim]HSO_4 [22], Triton X-100 in water [23], TiO_2 NPs [24], SnO_2 NPs [25], silica-bonded imidazolium-sulfonic acid chloride [26], [2-MPyH]OTf [27], SBA-15/SO_3H [28], Ni-nanoparticles [29], IL-HSO_4@SBA-15 [30], Baker's yeast [31], L-proline [32], and [bmim]BF_4 [33]. Although the reported methods offer several merits and provide improvements for the synthesis of the target molecules, many of these protocols need longer reaction times, hard reaction conditions, using unsafe organic solvents, and drastic workups. Therefore, surveying a newer environmentally compatible catalytic system is still in great demand.

In this effort, in order to explore a newer protocol to overpower the above mentioned difficulties in the way to the production of polyhydroquinoline derivatives and to continue our constant investigations on the knowledge-based maturation of the design, construction and applications of ionic liquids [34], molten salts [35], nano catalysts, magnetic nano particles (MNPs) [36], magnetic nano particles with ionic liquid tags [37], and trinitromethane [38] for organic functional group transformations, we wish to report the design, synthesis and applicability of a novel nano magnetically recoverable and reusable promoter catalyst namely $\{Fe_3O_4@SiO_2@(CH_2)_3Im\}C(NO_2)_3$ at the preparation of the polyhydroquinolines through a four component condensation of several arylaldehydes, dimedone, ethyl acetoacetate or methyl acetoacetate as *β*-ketoester, and ammonium acetate as a nitrogen source under mild and solvent free conditions (Schemes 1 and 2).

Characterization of the novel catalyst

The structural verification of the novel nano magnetically recoverable and reusable promoter namely $\{Fe_3O_4@SiO_2@(CH_2)_3Im\}C(NO_2)_3$ were made using appropriate technical skills such as FT-IR, X-ray diffraction patterns (XRD), field emission scanning electron microscopy (FESEM), elemental mapping, high resolution transmission electron microscopy (HRTEM), thermogravimetry (TG), and vibrating sample magnetometer (VSM) analysis.

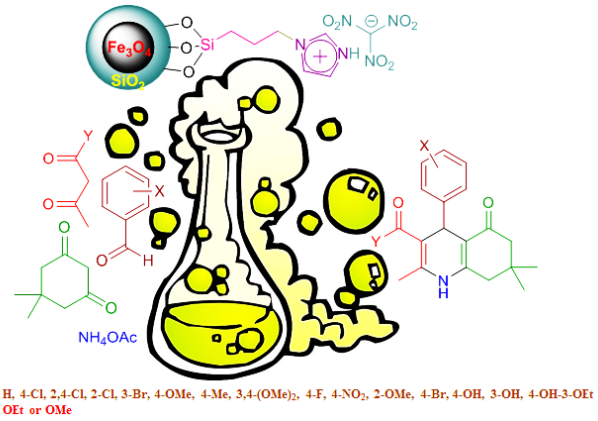

Scheme 1: Synthesis of polyhydroquinoline derivatives in the presence of $\{Fe_3O_4@SiO_2@(CH_2)_3Im\}C(NO_2)_3$

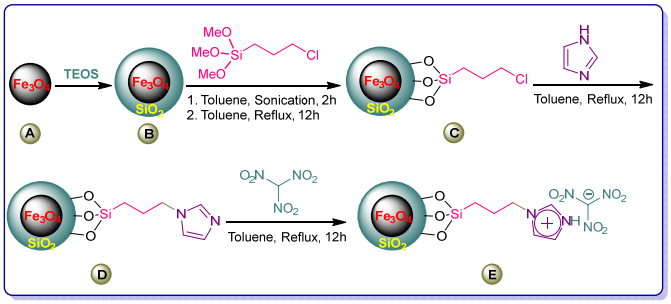

Scheme 2: Synthetic pathway for the preparation of $\{Fe_3O_4@SiO_2@(CH_2)_3Im\}C(NO_2)_3$ as a heterogeneous core-shell catalyst

As depicted in Fig. 2, the FT-IR spectrum of the novel nano magnetic heterogeneous core-shell catalyst in comparison with different step by step synthetic pathway compounds from $Fe_3O_4@SiO_2$ to $\{Fe_3O_4@SiO_2@(CH_2)_3Im\}C(NO_2)_3$ was investigated in the range of 400-4000 cm^{-1}. The overall differences in the FT-IR spectrums can be used as a proof for the preparation of the novel nano magnetically recoverable and reusable promoter catalyst. According to the FT-IR spectrum, the two peaks discerned at 1394 and 1592 cm^{-1} can be attributed to the nitro functional groups in the structure of the prepared catalyst. Furthermore, the overlapping of the uncoated hydroxyl groups and N-H stretching mode in the imidazolium ring has caused a broad peak in the region of about 2900-3700 cm^{-1}.

In a comparative manner, for the investigation of the purity and the phase of the applied materials for the synthesis of the presented catalyst, the X-ray diffraction patterns (XRD) of the different stepwise prepared materials were explored and the attained data were collected in Fig. 3. From the XRD patterns, it can be deduced that the addition of each layer to the surface of the Fe_3O_4

nanoparticles lead to a change compare with the previous stage which is an indication of the synthesis of the novel nano magnetic core-shell catalyst. The X-ray diffraction pattern of the prepared catalyst confirmed that it has a crystalline nature with diffraction lines at 2ϑ= 13.35°, 16.30° and 24.90°. In another study, according to the Scherrer equation D= $K\lambda/(\beta \cos \vartheta)$, where λ is the X-ray wavelength, K the Scherrer constant, β the peak width of half maximum and ϑ the Bragg diffraction angle, the XRD data comprising 2ϑ value, peak width, size of particles and interplanar distance, were extracted and embedded in Table 1.

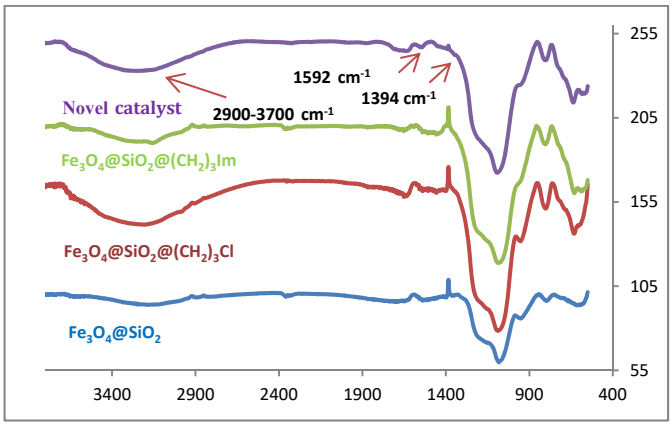

Fig. 2: FT-IR spectrum of the novel nano magnetic heterogeneous catalyst in comparison with different stepwise synthetic pathway materials

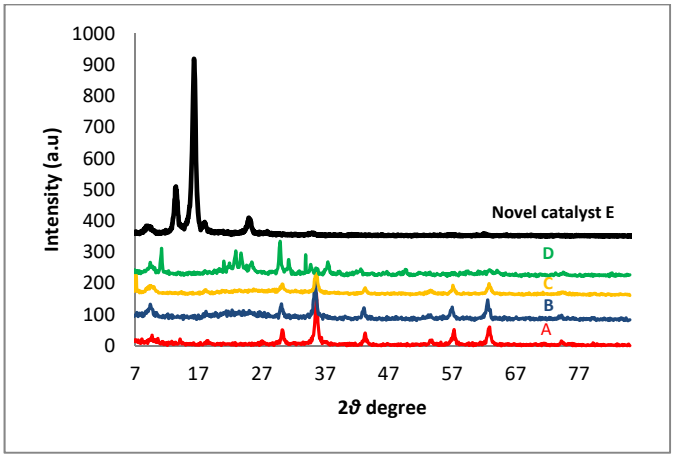

Fig. 3. XRD pattern of the new catalyst and comparison with the different stepwise synthesized intermediates.

Table 1: XRD extracted data related to novel presented nano magnetic catalyst

Entry	2ϑ	Peak width [FWHM] (degree)	Size [nm]	Inter planar distance [nm]
1	13.35	0.68	11.76	0.662439
2	16.30	0.64	12.54	0.543152
3	24.90	0.80	10.17	0.357164

In another assay, for the investigation of the size and morphology of the novel catalyst, field emission scanning electron microscopy (FESEM) images were obtained (Figures 4 a-c). As the recorded FESEM images show, the size of the catalyst particles is in the nanometer scale being between 19.6 and 53.7 nm.

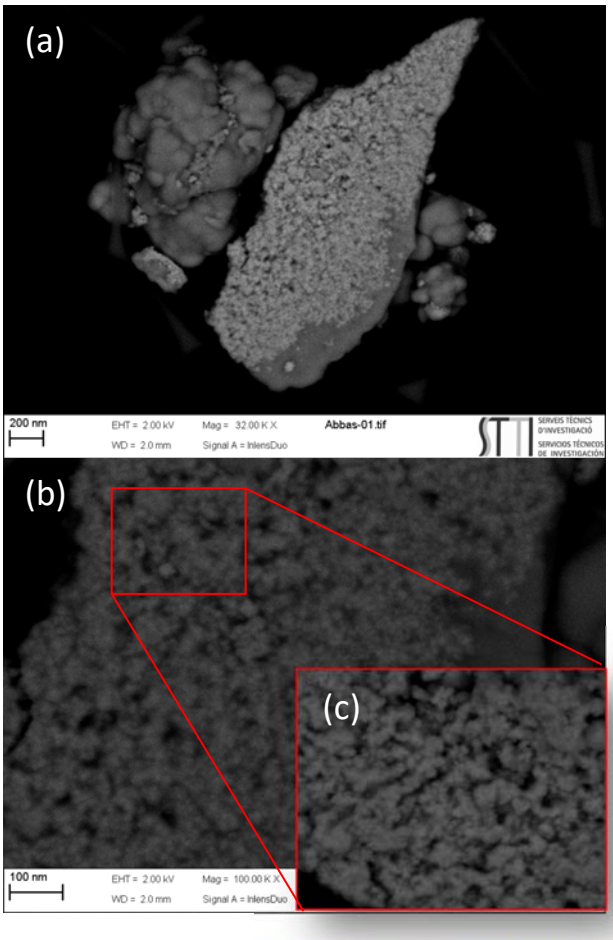

Fig. 4. (a,b) Field emission scanning electron microscope (FESEM) images of {Fe_3O_4@SiO_2@$(CH_2)_3$Im}C$(NO_2)_3$ as a new nano magnetic core-shell catalyst. Inset (c) expansion of image b.

Moreover, in order to explore the elemental composition of the catalyst {Fe_3O_4@SiO_2@$(CH_2)_3$Im}C$(NO_2)_3$, an energy-dispersive spectroscopy (EDS) elemental mapping analysis was conducted (Figure 5a-5g). Examination of the SEM-EDS mapping images, which are shown in Figures 5b-5g), proved the presence of Si, Fe, N, O, and C elements in the catalyst. As shown in Figures 5b-5f, the elements were well distributed in the catalyst surface.

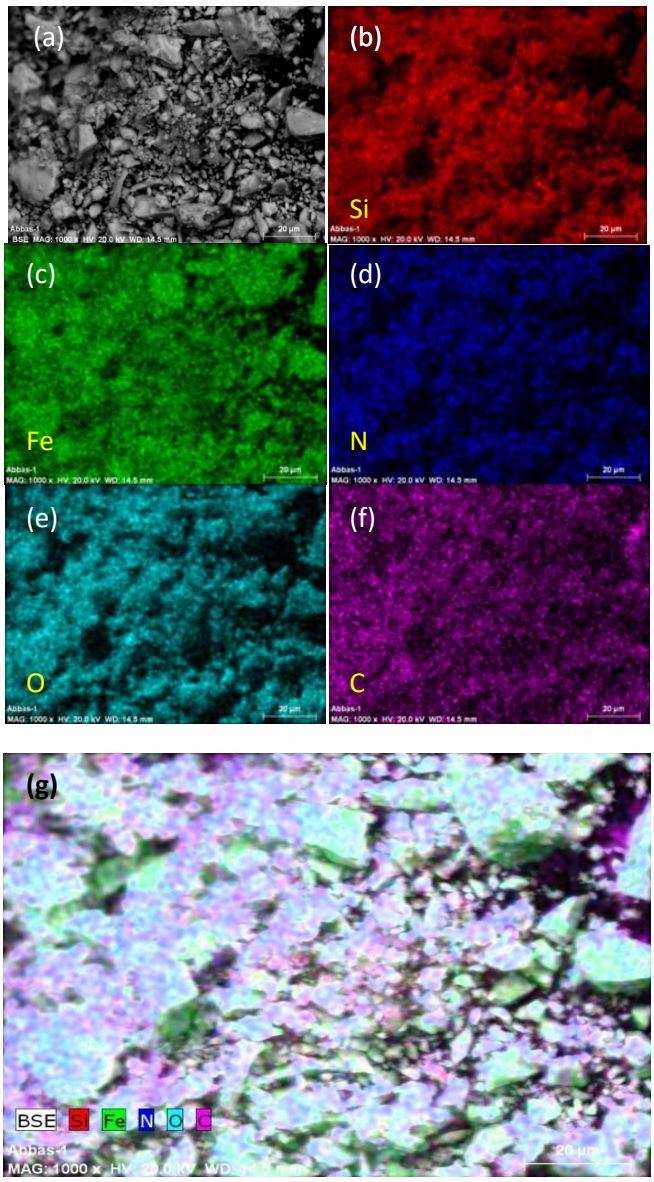

Fig. 5. (a) SEM image, and SEM-EDS elemental mapping images of (b) Silicon (red), (c) Iron (green), (d) Nitrogen (blue), (e) Oxygen (cyan), (f) Carbon (purple) and (g) overlapping of Si, Fe, N, O, C elements in $\{Fe_3O_4@SiO_2@(CH_2)_3Im\}C(NO_2)_3$

The collected data from energy dispersive X-ray (EDX) analysis of the new heterogeneous catalyst showed all predicted elements in the structure of the catalyst, namely iron, silicon, oxygen, carbon, and nitrogen as indicated in Figure 6. Besides, SEM-coupled EDX data for the presented catalyst derive that it derive C (0.53), N (.27), Fe (93.56), O (4.64) and Si (0.99).

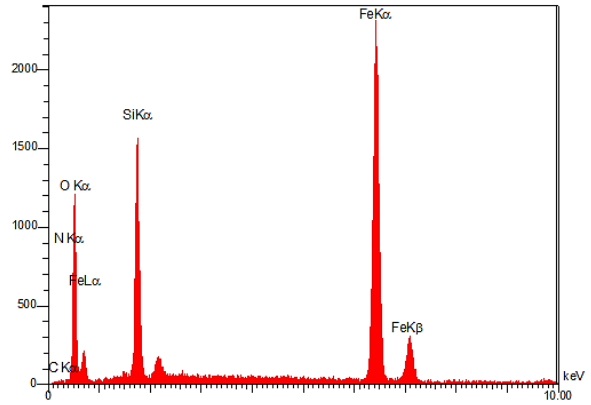

Fig. 6. Energy dispersive X-ray (EDX) spectrum of the new heterogeneous catalyst.

High Resolution transmission electron microscopy (HRTEM) images of $\{Fe_3O_4@SiO_2@(CH_2)_3Im\}C(NO_2)_3$ were recorded and illustrated to obtain in more detail structural information of the catalyst. As depicted in Figures 8a and 8b, all the nanoparticles presented well-defined uniform spherical shapes, highly dispersed by the ionic liquid tags over Fe_3O_4NPs after sonication in ethanol. As shown in the HRTEM image (Figures 8a-8c), amorphous silica coating layers over the crystalline nanoparticles of Fe_3O_4NPs are clearly revealed at low or high magnification of HRTEM. According to Fig. 8c, the thickness of silica shell ($@SiO_2@(CH_2)_3Im\}C(NO_2)_3$) is around 2 to 3 nm with an interplanar crystalline spacing value of Fe_3O_4NPs around 0.50 nm Figure 7. Moreover, it is worthy to mention that the obtained images from both FESEM and HRTEM analyses are in good agreement with XRD extracted data.

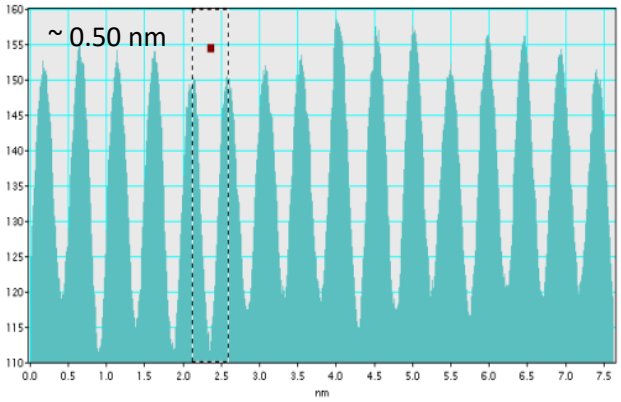

Fig. 7. Average of crystalline distance layer of Fe_3O_4NPs in $\{Fe_3O_4@SiO_2@(CH_2)_3Im\}C(NO_2)_3$

Journal Name

ARTICLE

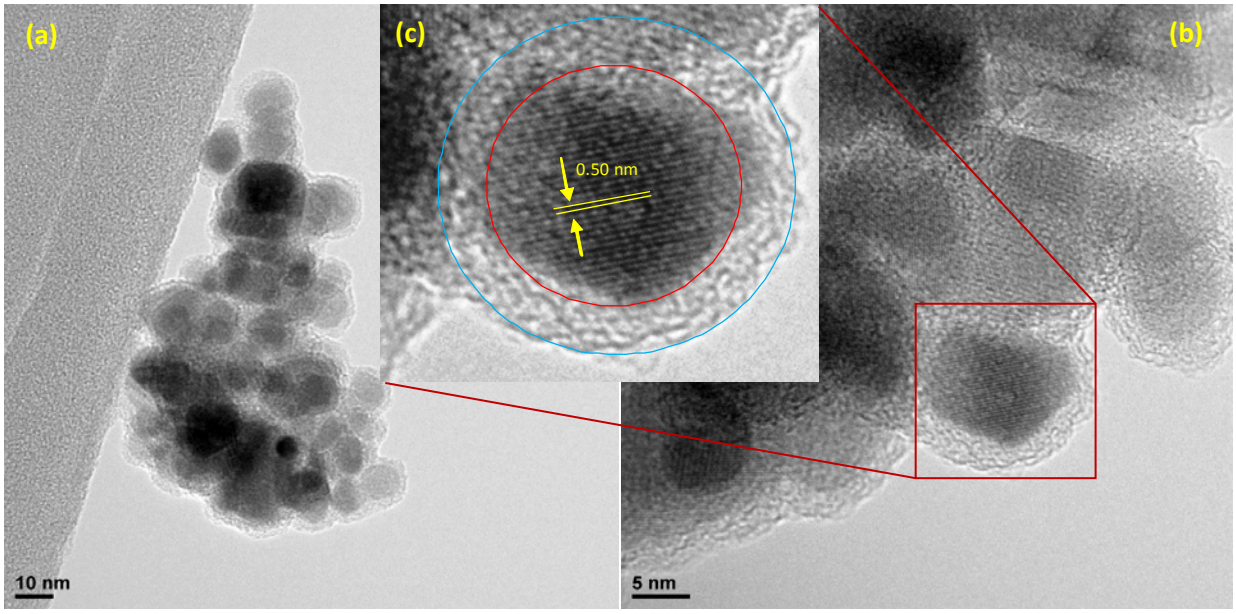

Fig. 8. HRTEM images of the {Fe_3O_4@SiO_2@$(CH_2)_3$Im}C$(NO_2)_3$ (a,b), and magnified HRTEM images of one nano particle (c).

In order to investigate the thermal stability of the novel nano magnetic catalyst, thermal gravimetric (TG), derivative thermal gravimetric (DTG), and differential thermal (DTA) analyses were conducted (Figure 9). From the performed studies, it could be inferred that the main weight loss upon heating from ambient temperature to about 100 °C can be attributed to the evaporation of the physically adsorbed water and other organic solvents used during the catalyst preparation. Weight loss at around 210 °C is due to thermal decomposition of the ionic tag of the catalyst. Finally, decomposition of the catalyst occurred between 300-550 °C. Also, the study of the DTA analysis diagram revealed that it is downward and exothermic.

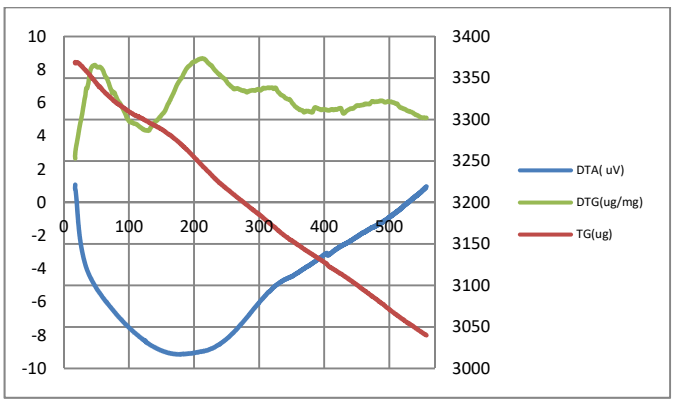

Fig. 9. Thermal gravimetric (TG), derivative thermal gravimetric (DTG), and differential thermal (DTA) analyses of the novel core-shell catalyst.

In another exploration and in order to study the magnetic properties of the new catalyst, the vibrating sample magnetometer (VSM) analysis of the catalyst was compared with nano magnetic Fe_3O_4 (Figure 10). By investigation the obtained magnetization curves data, it was disclosed that the saturation of the {Fe_3O_4@SiO_2@$(CH_2)_3$Im}C$(NO_2)_3$ as catalyst reduced from 52.42 emu g^{-1} for Fe_3O_4 nano particles to 37.48 emu g^{-1}. This decrease can be related to surface modification of the Fe_3O_4 nano particles during the preparation of the catalyst.

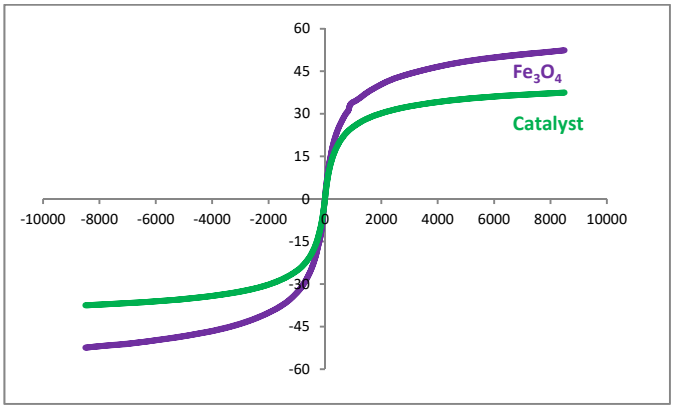

Fig. 10. VSM magnetization curves of catalyst compare with Fe_3O_4 nano particles

After approving of the presented nano magnetic catalyst using the aforementioned technical skills, the applicability of the described catalyst was explored for the synthesis of polyhydroquinoline derivatives through a four component condensation of several arylaldehydes, dimedone, ethyl acetoacetate or methyl acetoacetate as *β*-ketoester, and ammonium acetate as a nitrogen source. For this goal, and in order to achieve the optimized reaction conditions, the condensation of 4-chlorobenzaldehyde, dimedone, ethylacetoacetate, and ammonium acetate was picked up as test reaction. The resulting data for the optimization of temperatures, catalyst loadings, and solvents exhibited that the best results were acquired when the reaction was carried out under solvent-free conditions in the presence of 7 mg of $\{Fe_3O_4@SiO_2@(CH_2)_3Im\}C(NO_2)_3$ as catalyst at 80 °C (Table 2, Entry 4). The related obtained data for the optimization of the reaction conditions is included in Tale 2.

Table 2: Optimization of reaction conditions for the synthesis of polyhydroquinolines.[a]

Entry	Solvent	Load of catalyst (mg)	Temperature (°C)	Time (min)	Yield (%)[b]
1	-	10	100	15	93
2	-	10	80	16	92
3	-	10	60	25	85
4	**-**	**7**	**80**	**18**	**92**
5	-	4	80	22	87
6	-	-	80	60	54
7	EtOAc	7	Reflux	80	55
8	*n*-Hexane	7	Reflux	70	35
9	CH_3CN	7	Reflux	80	60
10	EtOH	7	Reflux	90	90
11	H_2O	7	Reflux	90	78

[a] Reaction conditions: 4-chlorobenzaldehyde (1 mmol, 0.144 g), dimedone (1 mmol, 0.140 g), ethyl acetoacetate (1 mmol, 0.130 g), ammonium acetate (3 mmol, 0.231 g). [b] Isolate yield.

After appraisal of the appropriate reaction conditions, we studied the scope and productivity of the presented process for the synthesis of biologically active target molecules in the presence of $\{Fe_3O_4@SiO_2@(CH_2)_3Im\}C(NO_2)_3$ as a heterogeneous recoverable catalyst. Thus, polyhydroquinoline derivatives were prepared *via* a four component reaction of a wide range of aromatic aldehydes bearing electron-withdrawing and electron-releasing groups, ethyl acetoacetate or methyl acetoacetate, dimedone, and ammonium acetate under solvent free conditions. The obtained results are displayed in Table 3.

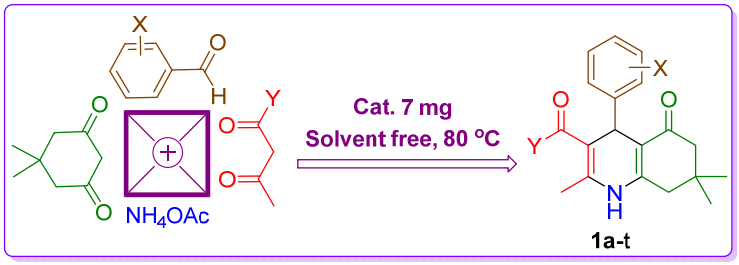

Table 3: Synthesis of the polyhydroquinolines in the presence of $\{Fe_3O_4@SiO_2@(CH_2)_3Im\}C(NO_2)_3$.[a]

Product	X	Y	Time (min)	Yield (%)[b]	M. p (°C) found [Lit][ref]
1a	4-Cl	OEt	18	92	243-245 [242-244][36c]

1b	H	OEt	19	91	224-226 [224-226] [36c]
1c	2,4-Cl_2	OEt	16	93	244-246 [242-244] [36c]
1d	4-OMe	OEt	18	90	255-257 [255-257][36c]
1e	3-Br	OEt	18	91	206-208[229-231][26]
1f	2-Cl	OEt	20	94	207-209 [208-209][39]
1g	4-Me	OEt	17	90	263-265 [263-265][36c]
1h	3,4-$(OMe)_2$	OEt	16	92	205-207 [204-206][36c]
1i	4-F	OEt	18	90	193-195 [193-195][36c]
1j	4-NO_2	OEt	22	88	242-243 [241-242][36c]
1k	2-OMe	OEt	14	92	249-251 [248-250][41]
1l	3-OEt-4-OH	OEt	15	95	195-196 [190-192][36c]
1m	3-OH	OEt	17	93	231-234 [230-232][36c]
1n	4-Cl	OMe	18	89	257-258 [219-222][40]
1o	H	OMe	17	90	259-261 [257-259][26]
1p	4-Br	OMe	19	90	261-263 [263-264][42]
1q	2,4-Cl	OMe	22	91	251-253 [250-252] [42]
1r	4-OMe	OMe	18	91	254-257 [256-259][26]
1s	4-OH	OMe	17	92	297-298 [232-234][26]
1t	4-Me	OMe	17	90	270-273 [283-285][23]

[a]Reaction conditions: aromatic aldehyde (1 mmol,), dimedone (1 mmol, 0.140 g), ethyl acetoacetate or methyl acetoacetate (1 mmol), ammonium acetate (3 mmol, 0.231g). [b] Isolated yields.

One of the excellent merits connected with nano magnetic heterogeneous core-shell catalysts is the recycling possibility and easy separation of them from the reaction mixture in a catalyzed system after completion of the reaction. In order to demonstrate the reusability of our catalyst, the reaction of benzaldehyde, dimedone, ethyl acetoacetate, and ammonium acetate was preferred as a model process. After performance of each run, hot ethanol was added to the reaction mixture to dissolve the crude product. Then, the nano magnetic catalyst was separated from the reaction mixture by applying an external magnet. The catalyst was reused for the next run after washing it with ethanol and drying. As depicted in Figure 11, the catalytic activity of {Fe_3O_4@SiO_2@$(CH_2)_3$Im}$C(NO_2)_3$ was conserved for eight consecutive runs without any discernible reduction.

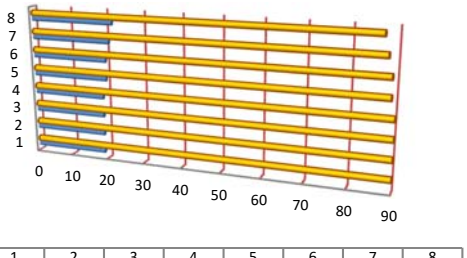

	1	2	3	4	5	6	7	8
Yield (%)	91	91	90	90	89	89	88	87
Time (min)	19	19	19	19	20	20	21	22

Fig. 11. Reusability test of the {Fe_3O_4@SiO_2@$(CH_2)_3$Im}$C(NO_2)_3$ as a novel nano magnetic catalyst

Finally, as embedded in Table 4, the catalytic activity of {Fe_3O_4@SiO_2@$(CH_2)_3$Im}$C(NO_2)_3$ was compared with some previously investigated recoverable catalysts. As depicted, it can be deduced that the previously reported methods suffer from

different drawbacks such as, elevated temperatures, use of organic solvents and/or transition metal catalyst, activation by sonication irradiation, longer reaction times, or harsh reaction conditions.

Table 4: Catalytic activity of presented nano magnetic catalyst compared with some other recoverable catalysts for the synthesis of compound **1b**

Entry	Reaction conditions	Time (min)	Yield (%)	Lit.
1	$[TBA]_2[W_6O_{19}]$ (7 mol%), Solvent-free, 110 °C	20	93	43
2	Trifluoroethanol (TFE), 70 °C	180	98	44
3	Fe_3O_4-SA-PPCA (10 mg), EtOH, 50 °C	120	97	45
4	Mn@PMO-IL (1 mol%), Solvent-free, 80 °C	20	95	46
5	Co_3O_4-CNTs (0.03 g), EtOH, 50 °C, Sonication	15	97	47
6	Nafion-H®, PEG 400-water (60:40), 50 °C	90	96	48
7	(bzacen)MnCl (2.5 mol%), EtOH, Reflux	20	90	49
8	Nano-Fe_3O_4 (5 mol%), Solvent-free, 50 °C	6	89	50
9	Nanocat Fe-Ce (100 mg), EtOH, r.t.	20	95	51
10	$Hf(NPf_2)_4$ (1 mol%), $C_{10}F_{18}$, 60 °C	180	95	52
This work	$\{Fe_3O_4@SiO_2@(CH_2)_3Im\}C(NO_2)_3$ (7 mg), Solvent-free, 80 °C	19	91	-

A suggested mechanistic pathway for the synthesis of polyhydroquinoline derivatives is portrayed in Figure 12, where initially the *in-situ* generated NH_3 form ammonium acetate reacts with activated *β*-ketoster to yield the corresponding intermediate **2**. On the other hand, in the presence of the novel nano magnetic catalyst, dimedone is converted to its enol form which performs a nucleophilic addition to the activated arylaldehyde, providing the corresponding knoevenagel adduct **3**. Then, the reaction between these two intermediates generates intermediate **4**. Tautomerization of **4** leads to the formation of derivative **5** which suffers an intramolecular nucleophilic attack of the amino group to the activated carbonyl group providing intermediate **6**. Finally, dehydration of this intermediate forms the desired target molecules **1a**-**t**.

Conclusion

In this study, the design and synthesis of a novel and heterogeneous reusable catalyst namely $\{Fe_3O_4@SiO_2@(CH_2)_3Im\}C(NO_2)_3$ has been reported. The structure of the presented catalyst was fully characterized using proper techniques such as, FT-IR, X-ray diffraction patterns (XRD), field emission scanning electron microscopy (FESEM), high Resolution transmission electron microscopy (HRTEM), thermogravimetry (TG), derivative thermal gravimetric (DTG), differential thermal (DTA), and vibrating sample magnetometer (VSM) analyses. The catalytic performance of $\{Fe_3O_4@SiO_2@(CH_2)_3Im\}C(NO_2)_3$ was successfully explored in the four component preparation of polyhydroquinoline derivatives under mild and eco-friendly reaction conditions. The encouraging points of this study are the eco-friendly and mild reaction conditions, easy separation and reusability of the catalyst, short reaction times with high products yields, and also easy work-up.

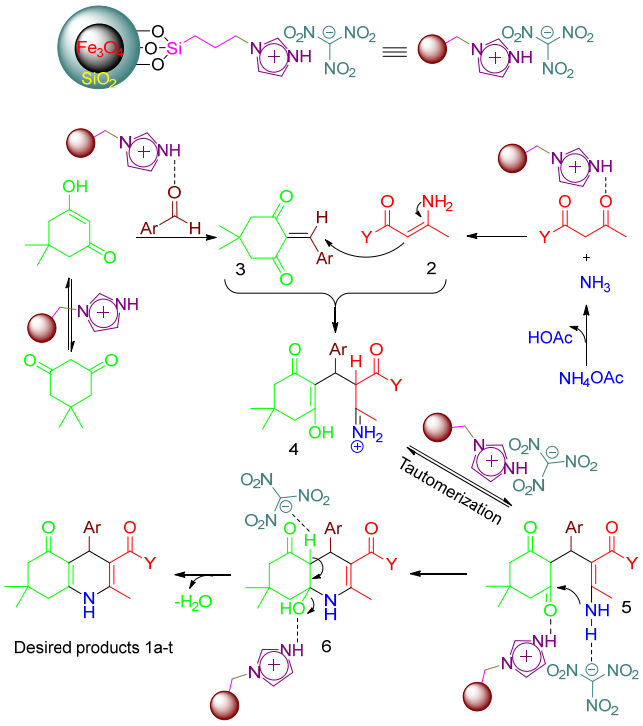

Fig. 12. Suggested catalytic mechanism for the synthesis of target molecules

Exprimental:

General

Solvents and reagents were purchased from Sigma- Aldrich, Alfa Aesar, and Merck and were used without further purification. Melting points were obtained with a Amstrad/electrothermal apparatus. ^1H NMR (400 MHz) and ^1H NMR (300 MHz) spectra were recorded on a Bruker Avance 400 and a Bruker Avance 300 NMR spectrometers, respectively, in proton coupled mode using, unless otherwise stated, deuterated DMSO as solvent. ^{13}C NMR (101 MHz) spectra were recorded on Bruker Avance 400 NMR spectrometer, in proton decoupled mode at 20 °C in deuterated DMSO as solvent, unless otherwise stated; chemical shifts are given in δ (parts per million) and the coupling constants (*J*) in Hertz. ^{19}F NMR (282 MHz) spectra were recorded on a Bruker Avance 300 NMR spectrometer, in proton coupled

mode. Infrared spectra were recorded with an FT-IR 4100 LE (JASCO, Pike Miracle ATR) spectrometer. HRTEM was carried out on a high Resolution transmission electron microscope JEOL JEM-2010. This microscope is equipped with an X-ray detector OXFORD INCA Energy TEM 100 for microanalysis (EDS). The acquisition of the images was performed using a GATAN ORIUS SC600 digital camera mounted on-axis, integrated with the program GATAN Digital Micrograph 1.80.70 for GMS 1.8.0. Field emission scanning electron microscope (FESEM) images were recorded on a Merlin VP Compact from Zeiss equipped with an EDS microanalysis system Quantax 400 from Bruker. The resolution was 0.8 nm at 15 kV and 1.6 nm at 1 kV. Field emission equipment is able to work at very reduced voltages (from 0.02 kV to 30 kV) allowing to observe beam sensitive samples without damaging them and minimizing the charging effects. Scanning electron microscope (SEM) studies were performed on a Hitachi S3000N, equipped with an X-ray detector Bruker XFlash 3001 for microanalysis (EDS) and mapping. The scanning microscope is able to work in variable pressure mode for observation of nonconductive specimens without coating with any conductive material. Low-resolution mass spectra (EI) were obtained at 70 eV with an Agilent 5973 Network spectrometer, with fragment ions m/z reported with relative intensities (%) in parentheses. HRMS analyses were carried out on Agilent 7200 (Q-TOF) spectrometers. Magnetic measurements were performed using vibration sample magnetometry VSM, (MDK Co. Kashan, Iran) analysis. TG-DTA analyses were carried out on a METTLER TOLEDO equipment, model TGA/SDTA851 and /SF/1100 TG-DTA. X-ray diffraction (XRD) analysis was performed using a Bruker D8-Advance apparatus with mirror Goebel (non-planar samples) equipped with a high temperature Chamber (up to 900°C), a generator of x-ray KRISTALLOFLEX K 760-80F (power: 3000W, voltage: 20-60KV and current: 5-80mA), and a tube of RX with copper anode. Preparative thin-layer chromatography was carried on laboratory made TLC glass plates with silica gel 60 PF254 (Merck). Column chromatography was performed using silica gel 60 of 40–60 microns (hexane/EtOAc as eluent).

Synthetic Procedures

General procedure for the preparation of novel silica-coated magnetic nanoparticles with tags of ionic liquid (Scheme 2)

At first, the Fe_3O_4 nanoparticles were synthesized according to a previously reported method [53]. Then, the surface of the Fe_3O_4 nano particles was modified with a layer of SiO_2 by treating with tetraethyl orthosilicate (TEOS) to form compound **B**. In the next step, silanization of the Fe_3O_4@SiO_2 (**B**) by reaction with 3-chloropropyltrimethoxysilane in refluxing toluene afforded compound **C**. Subsequently, 6 mmol (0.408 g) of imidazole was added to compound **C** dispersed in toluene. The resulting mixture was refluxed for 12 h. Finally, trinitromethane (6 mmol, 0.906 g) was added to compound **D** in toluene and the obtained reaction mixture was stirred for 12 h in refluxing toluene to form {Fe_3O_4@SiO_2@$(CH_2)_3$Im}$C(NO_2)_3$ (**E**) as a reusable nano magnetic core-shell catalyst with a ionic tag (Scheme 2).

General procedure for the synthesis of polyhydroquinolines as target molecules (Scheme 1)

To a round bottom flask containing a mixture of aromatic aldehyde (1 mmol), dimedone (1 mmol, 0.14 g), ethyl acetoacetate or methyl acetoacetate as *β*-ketoster (1 mmol), and ammonium acetate as a nitrogen source (3 mmol, 0.23 g), 7 mg of {Fe_3O_4@SiO_2@$(CH_2)_3$Im}$C(NO_2)_3$ were added as MNPs@IL catalyst. Then, the reaction mixture was stirred at 80 °C for adequate times under solvent-free conditions as embedded in Table 3. After accomplishment of the reactions, as monitored by TLC (*n*-hexane/ethyl acetate), the reaction mixture was cooled to ambient temperature. Afterwards, in order to separate and recover the catalyst, hot ethanol was added to the mixture to dissolve the desired products and un-reacted starting materials. The catalyst was insoluble in hot ethanol and easily separated from the reaction mixture by utilizing an external magnet. Finally, the target products were recrystallized from ethanol with high to excellent yields as inserted in Table 3.

Spectral data

Ethyl 4-(4-chlorophenyl)-2,7,7-trimethyl-5-oxo-1,4,5,6,7,8-hexahydroquinoline-3-carboxylate: (1a)[36c]
melting point: 243-245 °C; FT-IR (KBr): υ(cm^{-1}) = 3277, 3207, 3078, 2967, 1706, 1648, 1605, 1489, 1382, 1214; ^{1}H NMR (400 MHz) δ 9.08 (br. s, 1H), 7.22 (s, 2H), 7.14 (s, 2H), 4.82 (s, 1H), 3.95 (m, 2H), 2.45 (d, *J* = 17.0, 1H), 2.35-2.25 (m with s at 2.27, 4H), 2.15 (d, *J* = 15.5, 1H), 1.96 (d, *J* = 15.5, 1H), 1.10 (br. s, 3H), 0.99 (s, 3H), 0.81 (s, 3H); ^{13}C NMR (101 MHz) δ 194.7, 167.1, 150.0, 147.0, 145.8, 130.6, 129.7, 128.1, 110.1, 103.5, 59.5, 50.6, 36.0, 32.5, 29.5, 26.8, 18.7, 14.5; MS (EI) *m/z* (%): 375 (M^++2, 5), 373 (M^+, 14), 262.1 (100), 234 (20); TOF-HRMS (EI): *m/z* $(M)^+$ calcd for $C_{21}H_{24}ClNO_3$ 373.1445; found 373.1428.

Ethyl 2,7,7-trimethyl-5-oxo-4-phenyl-1,4,5,6,7,8-hexahydroquinoline-3-carboxylate: (1b) [36c]
melting point: 224-226 °C; FT-IR (KBr): υ(cm^{-1}) = 3289, 3216, 3081, 2962, 1701, 1614, 1485, 1382, 1212 ; ^{1}H NMR (400 MHz) δ 9.03 (br. s, 1H), 7.15 (s, 4H), 7.05 (s, 1H), 4.85 (s, 1H), 3.96 (m, 2H), 2.41 (d, *J* = 17.0, 1H), 2.35-2.20 (m with s at 2.27, 4H), 2.15 (d, *J* = 16.0, 1H), 1.96 (d, *J* = 16.0, 1H), 1.11 (s, 3H), 1.00 (s, 3H), 0.83 (s, 3H); ^{13}C NMR (101 MHz) δ 194.7, 167.3, 149.9, 148.1, 145.4, 128.1, 127.9, 126.1, 110.4, 104.1, 59.5, 50.7, 36.3, 32.6, 29.6, 26.9, 18.7, 14.6; MS (EI) *m/z* (%): 339 (M^+, 13), 262 (100), 234 (20); TOF-HRMS (EI): *m/z* $(M)^+$ calcd for $C_{21}H_{25}NO_3$ 339.1834; found 339.1863.

Ethyl 4-(2,4-dichlorophenyl)-2,7,7-trimethyl-5-oxo-1,4,5,6,7,8-hexahydroquinoline-3-carboxylate: (1c) [36c]
melting point: 244-246 °C; FT-IR (KBr): υ(cm^{-1}) = 3283, 3208, 3078, 2958, 1706, 1648, 1610, 1495; ^{1}H NMR (400 MHz) δ 9.11

(s, 1H), 7.33 (s, 1H), 7.27 (s, 2H), 5.14 (s, 1H), 3.93 (m, 2H), 2.41 (d, *J* = 17.1, 1H), 2.30-2.20 (m with s at 2.24, 4H), 2.13 (d, *J* = 16.1, 1H), 1.91 (d, *J* = 16.0, 1H), 1.07 (t, *J* = 6.8, 3H), 0.99 (s, 3H), 0.83 (s, 3H); ^{13}C NMR (101 MHz) δ 194.3, 167.0, 150.3, 145.9, 144.7, 133.3, 133.2, 131.2, 128.6, 127.3, 109.7, 103.2, 59.5, 50.6, 35.2, 32.4, 29.5, 26.8, 18.7, 14.5; MS (EI) *m/z* (%): 411 (M^++4, 1), 409 (M^++2, 5), 407 (M^+, 9), 372 (14), 262 (100), 234 (19); TOF-HRMS (EI): *m/z* $(M)^+$ calcd for $C_{21}H_{23}Cl_2NO_3$ 407.1055; found 407.1062.

Ethyl 4-(4-methoxyphenyl)-2,7,7-trimethyl-5-oxo-1,4,5,6,7,8-hexahydroquinoline-3-carboxylate: (1d) [36c]

melting point: 255-257 °C; FT-IR (KBr): υ(cm^{-1}) = 3277, 3202, 3078, 2957, 1701, 1649, 1606, 1496; ^{1}H NMR (400 MHz) δ 8.99 (s, 1H), 7.04 (d, *J* = 8.2, 2H), 6.73 (d, *J* = 8.2, 2H), 4.78 (s, 1H), 3.96 (q, *J* = 6.9, 2H), 3.66 (s, 3H), 2.40 (d, *J* = 17.0, 1H), 2.35-2.20 (m with s at 2.26, 4H), 2.15 (d, *J* = 16.0, 1H), 1.96 (d, *J* = 16.0, 1H), 1.13 (t, *J* = 6.9, 3H), 1.00 (s, 3H), 0.84 (s, 3H); ^{13}C NMR (101 MHz) δ 194.7, 167.4, 157.7, 149.6, 145.0, 140.5, 128.8, 113.5, 110.6, 104.4, 59.4, 55.3, 50.7, 35.4, 32.5, 29.6, 26.9, 18.7, 14.6; MS (EI) *m/z* (%): 369 (M^+, 33), 340 (13), 296 (11), 262 (100), 234 (21); TOF-HRMS (EI): *m/z* $(M)^+$ calcd for $C_{22}H_{27}NO_4$ 369.1940; found 369.1950.

Ethyl 4-(3-bromophenyl)-2,7,7-trimethyl-5-oxo-1,4,5,6,7,8-hexahydroquinoline-3-carboxylate: (1e)[26]

melting point: 206-208 °C; FT-IR (KBr): υ(cm^{-1}) = 3273, 3073, 2958, 1702, 1604, 1489, 1380, 1211, 1071, 769; ^{1}H NMR (400 MHz) δ 9.12 (s, 1H), 7.32 – 7.22 (m, 2H), 7.20 – 7.08 (m, 2H), 4.82 (s, 1H), 4.05-3.90 (m, 2H), 2.42 (d, *J* = 17.2, 1H), 2.38-2.25 (m with s at 2.29, 4H), 2.17 (d, *J* = 16.2, 1H), 1.99 (d, *J* = 15.8, 1H), 1.12 (t, *J* = 6.8, 3H), 1.00 (s, 3H), 0.85 (s, 3H); ^{13}C NMR (101 MHz) δ 194.7, 167.0, 150.7, 150.3, 146.0, 130.8, 130.5, 129.0, 127.0, 121.5, 109.9, 103.4, 59.6, 50.6, 36.5, 32.6, 29.5, 26.8, 18.8, 14.5; MS (EI) *m/z* (%): 419 (M^++ 2, 6), 417 (M^+, 6), 262 (100), 234 (23); TOF-HRMS (EI): *m/z* $(M)^+$ calcd for $C_{21}H_{24}BrNO_3$ 417.0940; found 417.0933.

Ethyl 4-(2-chlorophenyl)-2,7,7-trimethyl-5-oxo-1,4,5,6,7,8-hexahydroquinoline-3-carboxylate: (1f)[39]

melting point: 207-209 °C; FT-IR (KBr): υ(cm^{-1}) = 3277, 3210, 3073, 2957, 1701, 1649, 1606, 1496, 1380; ^{1}H NMR (400 MHz) δ 9.07 (s, 1H), 7.28 (d, *J* = 6.8, 1H), 7.24-7.12 (m, 2H), 7.06 (t, *J* = 7.0, 1H), 5.18 (s, 1H), 3.98-3.87 (m, 2H), 2.41 (d, *J* = 17.0, 1H), 2.32-2.20 (m with s at 2.24, 4H), 2.13 (d, *J* = 16.1, 1H), 1.91 (d, *J* = 16.1, 1H), 1.07 (t, *J* = 7.1, 3H), 1.00 (s, 3H), 0.84 (s, 3H); ^{13}C NMR (101 MHz) δ 194.3, 167.2, 150.1, 145.6, 145.4, 132.4, 131.9, 129.4, 127.7, 127.1, 110.0, 103.7, 59.4, 50.7, 35.4, 32.4, 29.6, 26.8, 18.6, 14.5; MS (EI) *m/z* (%): 375 (M^++2, 7), 373 (M^+, 22), 338 (39), 262 (100), 234 (48); TOF-HRMS (EI): *m/z* $(M)^+$ calcd for $C_{21}H_{24}ClNO_3$ 373.1445; found 373.1457.

Ethyl 2,7,7-trimethyl-5-oxo-4-(*p*-tolyl)-1,4,5,6,7,8-hexahydroquinoline-3-carboxylate: (1g) [36c]

melting point: 263-265 °C; FT-IR (KBr): υ(cm^{-1}) = 3276, 3208, 3078, 2958, 1702, 1648, 1606, 1493, 1282; ^{1}H NMR (400 MHz) δ 8.99 (s, 1H), 7.15-6.90 (m, 4H), 4.79 (s, 1H), 3.95 (m, 2H), 2.39 (d, *J* = 17.1, 1H), 2.36-2.10 (m with 2s at 2.25 and 2.18, 8H), 1.95 (d, *J* = 16.0, 1H), 1.12 (s, 3H), 0.99 (s, 3H), 0.83 (s, 3H); ^{13}C NMR (101 MHz) δ 194.7, 167.3, 149.8, 145.2 (2c), 135.0, 128.7, 127.8, 110.5, 104.2, 59.4, 50.7, 35.8, 32.6, 29.6, 26.9, 21.0, 18.7, 14.6; MS (EI) *m/z* (%): 353 (M^+, 18), 262 (100), 234 (18); TOF-HRMS (EI): *m/z* $(M)^+$ calcd for $C_{22}H_{27}NO_3$ 353.1991; found 353.2005.

Ethyl 4-(3,4-dimethoxyphenyl)-2,7,7-trimethyl-5-oxo-1,4,5,6,7,8-hexahydroquinoline-3-carboxylate: (1h) [36c]

melting point: 205-207 °C; FT-IR (KBr): υ(cm^{-1}) = 3280, 3213, 3081, 2941, 1696, 1605, 1514; ^{1}H NMR (300 MHz, EtOH-d_6) δ 6.80 (d, *J* = 1.2 Hz, 1H), 6.72-6.53 (m, 2H), 4.83 (s, 1H), 3.94 (q, *J* = 7.1, 2H), 3.66 (s, 3H), 3.63 (s, 3H), 2.35 (d, *J* = 17.0 Hz, 1H), 2.29-2.19 (m with s at 2.26, 4H), 2.13 (d, *J* = 16.4 Hz, 1H), 1.98 (d, *J* = 16.4 Hz, 1H), 1.09 (t, *J* = 7.1 Hz, 3H), 0.97 (s, 3H), 0.82 (s, 3H); ^{13}C NMR (101 MHz) δ 194.7, 167.3, 149.7, 148.3, 147.3, 144.9, 140.8, 119.6, 112.0, 111.8, 110.4, 104.2, 59.4, 55.7, 55.6, 50.6, 35.5, 32.5, 29.6, 26.8, 18.6, 14.6; MS (EI) *m/z* (%): 399 (M^+, 33), 370 (10), 262 (100), 234 (21); TOF-HRMS (EI): *m/z* $(M)^+$ calcd for $C_{23}H_{29}NO_5$ 399.2046; found 399.2056.

Ethyl 4-(4-fluorophenyl)-2,7,7-trimethyl-5-oxo-1,4,5,6,7,8-hexahydroquinoline-3-carboxylate: (1i) [36c]

melting point: 193-195 °C; FT-IR (KBr): υ(cm^{-1}) = 3291, 3219, 3078, 2959, 1702, 1607, 1487, 1382, 1212, 853, 531; ^{1}H NMR (400 MHz) δ 9.06 (s, 1H), 7.14 (m, 2H), 6.99 (m, 2H), 4.83 (s, 1H), 3.96 (m, 2H), 2.40 (d, *J* = 17.1, 1H), 2.34 – 2.20 (m with s at 2.28, 4H), 2.15 (d, *J* = 15.8, 1H), 1.96 (d, *J* = 15.9, 1H), 1.10 (s, 3H), 0.99 (s, 3H), 0.82 (s, 3H); ^{13}C NMR (101 MHz) δ 194.7, 167.2, 160.8 (d, *J* = 241.2), 149.9, 145.6, 144.3, 129.6 (d, *J* = 8.0), 114.8 (d, *J* = 21.0), 110.4, 103.9, 59.5, 50.6, 35.7, 32.6, 29.5, 26.9, 18.7, 14.6; MS (EI) *m/z* (%): 357 (M^+, 21), 262 (100), 234 (22); ^{19}F NMR (282 MHz, DMSO) δ -115.39; TOF-HRMS (EI): *m/z* $(M)^+$ calcd for $C_{21}H_{24}FNO_3$ 357.1740; found 357.1746.

Ethyl 2,7,7-trimethyl-4-(4-nitrophenyl)-5-oxo-1,4,5,6,7,8-hexahydroquinoline-3-carboxylate: (1j) [36c]

melting point: 242-243 °C; FT-IR (KBr): υ(cm^{-1}) = 3274, 3189, 3076, 2966, 1703, 1649, 1609, 1493, 1349, 1215; ^{1}H NMR (400 MHz) δ 9.22 (s, 1H), 8.09 (d, *J* = 8.5, 2H), 7.41 (d, *J* = 8.5, 2H), 4.96 (s, 1H), 3.96 (q, *J* = 6.9, 2H), 2.43 (d, *J* = 17.1, 1H), 2.35-2.25 (m with s at 2.31, 4H), 2.18 (d, *J* = 16.2, 1H), 1.97 (d, *J* = 16.2, 1H), 1.10 (t, *J* = 7.0, 3H), 1.00 (s, 3H), 0.81 (s, 3H); ^{13}C NMR (101 MHz) δ 194.7, 166.8, 155.4, 150.5, 146.6, 146.1, 129.2, 123.6, 109.5, 102.8, 59.7, 50.5, 37.1, 32.6, 29.4, 26.9, 18.8, 14.5; MS (EI) *m/z* (%): 384 (M^+, 15), 262 (100), 234 (22); TOF-HRMS (EI): *m/z* $(M)^+$ calcd for $C_{21}H_{24}N_2O_5$ 384.1685; found 384.1692.

Ethyl 4-(2-methoxyphenyl)-2,7,7-trimethyl-5-oxo-1,4,5,6,7,8-hexahydroquinoline-3-carboxylate: (1k)[41]

melting point: 249-251 °C; FT-IR (KBr): υ(cm^{-1}) = 3284, 3078, 2964, 1689, 1623, 1611, 1488, 1361, 1215, 751; ^{1}H NMR (300 MHz, EtOH-d_6) δ 7.15 (d, *J* = 7.0, 1H), 6.93 (t, *J* = 7.4, 1H), 6.79-6.56 (m, 2H), 5.06 (s, 1H), 3.87 (q, *J* = 7.0, 2H), 3.65 (s, 3H), 2.32 (d, *J* = 17.0, 1H), 2.26-2.15 (m with s at 2.18, 4H), 2.14-1.97 (m, 1H), 1.91 (d, *J* = 16.4, 1H), 1.10-0.90 (m, 6H), 0.80 (s, 3H); ^{13}C NMR (101 MHz) δ 193.8, 167.3, 157.1, 149.9, 144.1, 134.9, 130.5, 126.9, 119.4, 111.0, 108.6, 102.9, 58.7, 55.1, 50.4, 32.8, 32.0, 29.3, 26.2, 18.0, 14.1; MS (EI) *m/z* (%): 369 (M^+, 61), 340 (37), 262 (100), 234 (31); TOF-HRMS (EI): *m/z* $(M)^+$ calcd for $C_{22}H_{27}NO_4$ 369.1940; found 369.1946.

Ethyl 4-(3-ethoxy-4-hydroxyphenyl)-2,7,7-trimethyl-5-oxo-1,4,5,6,7,8-hexahydroquinoline-3-carboxylate: (1l)[36c]

melting point: 195-196 °C; FT-IR (KBr): υ(cm^{-1}) = 3443, 3282, 3200, 3079, 2959, 1657, 1616, 1493, 1381; ^{1}H NMR (300 MHz, EtOH-d_6) δ 6.74 (s, 1H), 6.52 (s, 2H), 4.79 (s, 1H), 4.02-3.81 (m, 4H), 2.33 (d, *J* = 17.0, 1H), 2.28-2.18 (m with s at 2.25, 4H), 2.12 (d, *J* = 16.5, 1H), 1.98 (d, *J* = 16.4, 1H), 1.27 (t, *J* = 7.0, 3H), 1.08 (t, *J* = 7.1, 3H), 0.96 (s, 3H), 0.81 (s, 3H); ^{13}C NMR (101 MHz) δ 194.8, 167.4, 149.6, 146.2, 145.3, 144.8, 139.4, 120.1, 115.4, 113.9, 110.6, 104.5, 64.2, 59.4, 50.7, 35.4, 32.5, 29.6, 26.8, 18.7, 15.2, 14.6; MS (EI) *m/z* (%): 399 (M^+, 30), 370 (11), 262 (100),

234 (19); TOF-HRMS (EI): *m/z* $(M)^+$ calcd for $C_{23}H_{29}NO_5$ 399.2046; found 399. 2048.

Ethyl 4-(3-hydroxyphenyl)-2,7,7-trimethyl-5-oxo-1,4,5,6,7,8-hexahydroquinoline-3-carboxylate: (1m) [36c]

melting point: 231-234 °C; FT-IR (KBr): υ(cm^{-1}) = 3463, 3291, 2961, 1669, 1620, 1487, 1381, 1277, 1216; ^{1}H NMR (400 MHz) δ 9.05 (s, 1H), 9.00 (s, 1H), 6.94 (t, *J* = 7.7, 1H), 6.59-6.56 (m, 2H), 6.45 (d, *J* = 7.3, 1H), 4.78 (s, 1H), 3.98 (q, *J* = 7.0, 2H), 2.40 (d, *J* = 17.0, 1H), 2.32-2.25 (m with s at 2.27, 4H), 2.16 (d, *J* = 16.1, 1H), 1.99 (d, *J* = 16.1, 1H), 1.14 (t, *J* = 7.1, 3H), 1.00 (s, 3H), 0.87 (s, 3H); ^{13}C NMR (101 MHz) δ 194.7, 167.4, 157.3, 149.9, 149.4, 145.1, 128.9, 118.6, 115.0, 113.1, 110.4, 104.1, 59.5, 50.8, 36.1, 32.5, 29.6, 27.0, 18.7, 14.6; MS (EI) *m/z* (%): 355 (M^+, 13), 262 (100), 234 (20); TOF-HRMS (EI): *m/z* $(M)^+$ calcd for $C_{21}H_{25}NO_4$ 355.1784; found 355.1792.

Methyl 4-(4-chlorophenyl)-2,7,7-trimethyl-5-oxo-1,4,5,6,7,8-hexahydroquinoline-3-carboxylate: (1n)[40]

melting point: 257-258 °C; FT-IR (KBr): υ(cm^{-1}) = 3288, 3198, 3076, 1682, 1606, 1492, 1226; ^{1}H NMR (400 MHz) δ 9.12 (s, 1H), 7.23 (br. d, *J* = 6.6, 2H), 7.13 (br. d, *J* = 6.4, 2H), 4.83 (s, 1H), 3.51 (s, 3H), 2.40 (d, *J* = 17.0, 1H), 2.35-2.20 (m with s at 2.28, 4H), 2.16 (d, *J* = 16.0, 1H), 1.96 (d, *J* = 15.7, 1H), 0.99 (s, 3H), 0.81 (s, 3H); ^{13}C NMR (101 MHz) δ 194.7, 167.6, 150.0, 146.8, 146.1, 130.7, 129.6, 128.2, 110.1, 103.2, 51.1, 50.6, 35.8, 32.6, 29.5, 26.8, 18.8; MS (EI) *m/z* (%): 361 (M^++2, 4), 359 (M^+, 11), 248 (100); TOF-HRMS (EI): *m/z* $(M)^+$ calcd for $C_{20}H_{22}ClNO_3$ 359.1288; found 359.1275.

Methyl 2,7,7-trimethyl-5-oxo-4-phenyl-1,4,5,6,7,8-hexahydroquinoline-3-carboxylate: (1o)[26]

melting point: 259-261 °C; FT-IR (KBr): υ(cm^{-1}) = 3278, 3202, 3079, 2986, 1709, 1607, 1789, 1309; ^{1}H NMR (300 MHz, EtOH-d_6) δ 7.13 (d, *J* = 7.3, 2H), 7.02 (t, *J* = 7.4, 2H), 6.92 (t, *J* = 7.1, 1H), 4.89 (s, 1H), 3.53 (s, 3H), 2.34 (d, *J* = 17.0, 1H), 2.28-2.18 (m with s at 2.26, 4H) , 2.12 (d, *J* = 16.5, 1H), 1.97 (d, *J* = 16.5, 1H), 0.96 (s, 3H), 0.79 (s, 3H); ^{13}C NMR (101 MHz) δ 194.7, 167.7, 149.9, 147.9, 145.7, 128.2, 127.7, 126.1, 110.4, 103.6, 51.1, 50.7, 36.0, 32.6, 29.6, 26.8, 18.7; MS (EI) *m/z* (%): 325 (M^+, 11), 248 (100); TOF-HRMS (EI): *m/z* $(M)^+$ calcd for $C_{20}H_{23}NO_3$ 325.1678; found 325.1673.

Methyl 4-(4-bromophenyl)-2,7,7-trimethyl-5-oxo-1,4,5,6,7,8-hexahydroquinoline-3-carboxylate: (1p)[42]

melting point: 261-263 °C; FT-IR (KBr): υ(cm^{-1}) = 3291, 3202, 3078, 2958, 1683, 1606, 1492, 1382, 1332, 1227; ^{1}H NMR (300 MHz, EtOH-d_6) δ 7.17 (d, *J* = 8.3, 2H), 7.05 (d, *J* = 8.3, 2H), 4.85 (s, 1H), 3.47 (s, 3H), 2.34 (d, *J* = 17.0, 1H), 2.30-2.19 (m with s at 2.27, 4H), 2.12 (d, *J* = 16.4, 1H), 1.98 (d, *J* = 16.6, 1H), 0.96 (s, 3H), 0.79 (s, 3H); ^{13}C NMR (101 MHz) δ 194.7, 167.5, 150.1, 147.2, 146.1, 131.1, 130.0, 119.2, 110.0, 103.1, 51.2, 50.6, 35.6, 32.6, 29.5, 26.9, 18.8; MS (EI) *m/z* (%): 405 (M^++2, 7), 403 (M^+, 7), 248 (100); TOF-HRMS (EI): *m/z* $(M)^+$ calcd for $C_{20}H_{22}BrNO_3$ 403.0783; found 403.0674.

Methyl 4-(2,4-dichlorophenyl)-2,7,7-trimethyl-5-oxo-1,4,5,6,7,8-hexahydroquinoline-3-carboxylate: (1q)[42]

melting point: 251-253 °C; FT-IR (KBr): υ(cm^{-1}) = 3416, 3263, 1378, 2957, 1710, 1650, 1588, 1493, 1216; ^{1}H NMR (300 MHz, EtOH-d_6) δ 7.21 (d, *J* = 8.3, 1H), 7.09 (d, *J* = 1.8, 1H), 7.01 (dd, *J* = 8.3, 1.7, 1H), 5.19 (s, 1H), 3.43 (s, 3H), 2.35 (d, *J* = 17.0, 1H), 2.30-2.15 (m with s at 2.21, 4H), 2.10 (d, *J* = 16.4, 1H), 1.93 (d, *J* = 16.3, 1H), 0.97 (s, 3H), 0.83 (s, 3H); ^{13}C NMR (101 MHz) δ 194.4, 167.5, 150.3, 146.0, 144.9, 133.2, 132.9, 131.2, 128.6, 127.4, 109.9, 100.5, 50.9, 50.6, 35.0, 32.5, 29.5, 26.8, 18.6; MS (EI) *m/z* (%): 397 (M^++4, 1), 395 (M^++2, 5), 393 (M^+, 7), 358 (15), 248 (100); TOF-HRMS (EI): *m/z* $(M)^+$ calcd for $C_{20}H_{21}Cl_2NO_3$ 393.0898; found 393.0910.

Methyl 4-(4-methoxyphenyl)-2,7,7-trimethyl-5-oxo-1,4,5,6,7,8-hexahydroquinoline-3-carboxylate: (1r)[26]

melting point: 254-257 °C; FT-IR (KBr): υ(cm^{-1}) = 3188, 3067, 2961, 1705, 1649, 1605, 1498; ^{11}H NMR (300 MHz, EtOH-d_6) δ 7.03 (d, *J* = 8.1, 2H), 6.58 (d, *J* = 8.1, 2H), 4.82 (s, 1H), 3.59 (s, 3H), 3.46 (s, 3H), 2.33 (d, *J* = 17.0, 1H), 2.28-2.16 (m with s at 2.25, 4H), 2.12 (d, *J* = 16.5, 1H), 1.97 (d, *J* = 16.5, 1H), 0.96 (s, 3H), 0.80 (s, 3H); ^{13}C NMR (101 MHz) δ 194.7, 167.8, 157.7, 149.6, 145.4, 140.3, 128.6, 113.6, 110.7, 104.0, 55.3, 51.1, 50.7, 35.2, 32.6, 29.6, 26.9, 18.7; MS (EI) *m/z* (%): 355.2 (M^+, 26), 248.1 (100); TOF-HRMS (EI): *m/z* $(M)^+$ calcd for $C_{21}H_{25}NO_4$ 355.1784; found 355.1788.

Methyl 4-(4-hydroxyphenyl)-2,7,7-trimethyl-5-oxo-1,4,5,6,7,8-hexahydroquinoline-3-carboxylate: (1s)[26]

melting point: 297-298 °C; FT-IR (KBr): υ(cm^{-1}) = 3400, 3276, 3199, 2960, 1687, 1611, 1487, 1380, 1222, 1168, 768; ^{1}H NMR (300 MHz, EtOH-d_6) δ 6.93 (d, *J* = 8.1 Hz, 2H), 6.49 (d, *J* = 8.1 Hz, 2H), 4.79 (s, 1H), 3.47 (s, 3H), 2.33 (d, *J* = 17.0 Hz, 1H), 2.22 (m with s at 2.25, 4H), 2.11 (d, *J* = 16.5 Hz, 1H), 1.97 (d, *J* = 16.5 Hz, 1H), 0.96 (s, 3H), 0.80 (s, 3H); ^{13}C NMR (101 MHz) δ 194.3, 167.5, 155.2, 149.1, 144.7, 138.2, 128.1, 114.5, 110.4, 103.7, 50.6, 50.3, 34.5, 32.1, 29.1, 26.4, 18.2; MS (EI) *m/z* (%): 341 (M^+, 23), 248 (100); TOF-HRMS (EI): *m/z* $(M)^+$ calcd for $C_{20}H_{23}NO_4$ 341.1627; found 341.1628.

Methyl 2,7,7-trimethyl-5-oxo-4-(p-tolyl)-1,4,5,6,7,8-hexahydroquinoline-3-carboxylate: (1t)[23]

melting point: 270-273 °C; FT-IR (KBr): υ(cm^{-1}) = 3191, 3072, 2958, 1686, 1644, 1503, 1491, 1227; ^{1}H NMR (300 MHz, EtOH-d_6) δ 7.01 (d, *J* = 7.8, 2H), 6.83 (d, *J* = 7.6, 2H), 4.84 (s, 1H), 3.47 (s, 3H), 2.33 (d, *J* = 16.7, 1H), 2.27-2.19 (m with s at 2.25, 4H), 2.15-1.90 (m with s at 2.11, 5H), 0.96 (s, 3H), 0.80 (s, 3H); ^{13}C NMR (101 MHz) δ 194.7, 167.8, 149.7, 145.5, 145.0, 135.0, 128.8, 127.6, 110.5, 103.8, 51.0, 50.7, 35.6, 32.5, 29.6, 26.9, 21.0, 18.7; MS (EI) *m/z* (%): 339 (M^+, 15), 248 (100); TOF-HRMS (EI): *m/z* $(M)^+$ calcd for $C_{21}H_{25}NO_3$ 339.1834; found 339.1834.

Acknowledgements

We thank Bu-Ali Sina University, Iran National Science Foundation (INSF) (Allameh Tabataba'i's Award, Grant Number BN093), University of Alicante (VIGROB-173), and the Spanish Ministerio de Economía y Competitividad (CTQ2015-66624-P) for financial support to our research groups.

Reference

[1] T. Cheng, D. Zhang, H. Li and G. Liu, *Green Chem*., 2014, **16**, 3401.

[2] (a) D. Zhang, C. Zhou, Z. Sun, L. Z. Wu, C. H. Tung and T. Zhang, *Nanoscale*, 2012, **4**, 6244., (b) B. Karimi, F. Mansouri and H. M. Mirzaei, *ChemCatChem* 2015, **7**, 1736.

[3] (a) S. Ganesh Babu, R. Karvembu, *Catal. Surv. Asia*, 2013, **17**, 156., (b) D. Zhang, C. Zhou, Z. Sun, L. Z. Wu, C. H. Tung, T. Zhang, *Nanoscale*, 2012, **4**, 6244., (c) V. Polshettiwar, R. Luque, A. Fihri, H. Zhu, M. Bouhrara, J. M. Basset, *Chem. Rev*. 2011, **111**, 3036., (d) S. Shylesh, V. Schunemann, W. R. Thiel, *Angew. Chem. Int. Ed.* 2010, **49**, 3428., (e) S. Laurent, D. Forge, M. Port, A. Roch, C.

Robic, L.V. Elst, R.N. Muller, *Chem. Rev.* 2008, 108, 2064-2110. (f) A.H. Lu, E.L. Salabas, F. Schìth, *Angew. Chem. Int. Ed*. 2007, **46**, 1222.,(g) R. Hudson, Y. Feng, R. S. Varma, A. Moores, *Green Chem*., 2014, **16**, 4493. (g) M. Mokhtary, *J. Iran. Chem. Soc.* 2016, DOI 10.1007/s13738-016-0900-4

[4] M. Vafaeezadeh, H. Alinezhad, *J. Mol. Liq.* 2016, **218**, 95.

[5] Y. Gua, and G. Li, *Adv. Synth. Catal*. 2009, **351**, 817.

[6] C. Yue, D. Fang, L, Liu, T. F. Yi, *J. of Mol. Liq.* 2011, **163**, 99.

[7] T. L. Greaves and C. J. Drummond, *Chem. Rev*. 2008, **108**, 206.

[8] J. P. Hallett and T. Welton, *Chem. Rev.* 2011, **111**, 3508.

[9] M. Smiglak, J. M. Pringle, X. Lu, L. Han, S. Zhang, H. Gao, D. R. MacFarlane and R. D. Rogers DOI: 10.1039/c4cc02021a.

[10] (a) Q. Zhang, S. Zhang and Y. Deng, *Green Chem*., 2011, **13**, 2619, (b) F. Dong, F. Zhenghao, L. Zuliang, *Catal. Commun.*, 2009, **10**, 1267, (c) E. S. Putilova, G. V. Kryshtal, G. M. Zhdankina, N. A. Troitskii, and S. G. Zlotin, *Russ. J. Org. Chem.* 2005, **41**, 512.

[11] K. S. Egorova and V. P. Ananikov, *ChemSusChem*, 2014, **7**, 336.

[12] T. P. T. Pham, C. W. Cho, Y. S. Yun, *Water Res.*, 2010, **44**, 352.

[13] Z. Zarnegar and J. Safari, *J. Nanopart. Res*., 2014, **16**, 1.

[14] Multicomponent Reactions; Zhu, J.; Bienayme, H., Eds.; Wiley-VCH: Weinheim, 2005.

[15], A. Domling, I. Ugi, *Angew. Chem. Int. Ed*. 2000, **39**, 3169.

[16] J. E. Biggs-Houck, A. Younai and J. T Shaw, *Curr. Opin. Chem. Biol.* 2010, **14**, 371.

[17] R. P. Gore, A. P. Rajput, *drug invention today*, 2013, **5**, 148.

[18] A. Heydari, S. Khaksar, M. Tajbakhsh, R. Bijanzadeh, *J. Fluor. Chem.* 2009, **130**, 609.

[19] (a) P. P. Ghosh, P. Mukherjee and A. R. Das, *RSC Adv*., 2013, **3**, 8220, (b) B. H. Rotstein, S. H. Liang, V. V. Belov, E. Livni, D. B. Levine, A. A. Bonab, M. I. Papisov, R. H. Perlis and N. Vasdev, *Molecules* 2015, **20**, 9550., (c) A. Kumar and S. Sharma, *Green Chem*., 2011, **13**, 2017., (d) C. O. Okoro, M. A. Ogunwale and T. Siddiquee, *Appl*. *Sci*. 2012, **2**, 368.

[20] C. G. Evans, U. K. Jinwal, L. N. Makley, C. A. Dickey and J. E. Gestwicki, *Chem*. *Commun*., 2011, **47**, 529.

[21] D. Zhang, L. Z. Wu, L. Zhou, X. Han, Q. Z. Yang, L. P. Zhang and C. H. Tung, *J. Am. Chem. Soc*., 2004, **126**, 3440.

[22] A. Khazaei, M. A. Zolfigol, A. R. Moosavi-Zare, J. Afsar, A. Zare, V. Khakyzadeh and M. H. Beyzavi, *Chinese J. Catal*., 2013, **34**, 1936.

[23] M. R. Poor Heravi , S. Mehranfar, N. Shabani, *C. R. Chimie*, 2014, **17**, 141.

[24] M. Tajbakhsh, E. Alaee, H. Alinezhad, M. Khanian, F. Jahani, S. Khaksar, P. Rezaee and M. Tajbakhsh, *Chin. J. Catal*., 2012, **33**, 1517.

[25] S. M. Vahdat, F. Chekin, M. Hatami, M. Khavarpour, S. Baghery and Z. Roshan-Kouhi, *Chin. J. Catal*., 2013, **34**, 758.

[26] A. R. Moosavi-Zare, M. A. Zolfigol, M. Zarei, A. Zare and Javad Afsar, *Appl. Catal. A.: Gen.* 2015, 505, 224.

[27] M. Tajbakhsh, A. Alinezhad, M. Norouzi, S. Baghery and M. Akbari, *J. Mol. Liq.,* 2013, **177**, 44.

[28] S. Rostamnia, H. Xin, X. Liu, K. Lamei, *J. Mol. Catal. A: Chem.,* 2013, **374**, 85.

[29] S. B. Sapkal, K. F. Shelke, B. B. Shingate and M. S. Shingare, *Tetrahedron Lett*., 2009, **50**, 1754.

[30] S. Rostamnia, A. Hassankhani, H. Golchin, H. Behnam Gholipour, H. Xin, *J. Mol. Catal. A: Chem.,* 2014, **395**, 463.

[31] A. Kumar and R. A. Maurya, *Tetrahedron Lett*., 2007, **48**, 3887.

[32] N. N. Karade, V. H. Budhewar, S. V. Shinde and W. N. Jadhav, *Lett. Org. Chem*., 2007, **4**, 16.

[33] S. J. Ji, Z. Q. Jiang, J. Lu and T. P. Loh, *Synlett*, 2004, 831.

[34] E. Kianpour, S. Azizian, M. Yarie, M. A. Zolfigol, M. Bayat, *Chem. Eng. J.,* **295**, 500., (2016). And references cited therein.

[35] (a) M. A. Zolfigol, N. Mansouri, S. Baghery, *Synlett,* 2016, **27**, 1511.,(b) M. A. Zolfigol, M. Yarie, S. Baghery, *Synlett.* 2016, **27**, 1418.,(c) M. A. Zolfigol, N. Bahraminezhad S. Baghery, *J. Mol. Liq.,* 2016, **218**, 558., (d) M. A. Zolfigol, S. Baghery, A. R. Moosavi-Zare, S. M. Vahdat, H., *J. Mol. Catal. A: Chem.,* 2015*,* **409***,* 216. And references cited therein.

[36] a) T. Azadbakht, M. A. Zolfigol, R. A., V. Khakyzadeh and D. M. Perrin, *New J.Chem*., 2015, **39**, 439; (b) M. A. Zolfigol, T. Azadbakht, V. Khakyzadeh, R. Nejatyami and D. M. Perrin, *RSC Adv*., 2014, **4**, 40036., (c) M. A. Zolfigol, V. Khakyzadeh, A. R. Moosavi-Zare, A. Rostami, A. Zare, N. Iranpoor, M. H. Beyzavie and R. Luque, *Green Chem*., 2013, **15**, 2132., (d) N. Koukabi, E. Kolvari, A. Khazaei, M. A. Zolfigol, B. Shirmardi-Shaghasemi, H. R. Khavasi, *Chem. Commun*., 2011, **47**, 9230., (e) M. A. Zolfigol, R. Ayazi-Nasrabadi, S. Baghery, V. Khakyzadeh, S. Azizian, *J. Mol Catal. A: Chem.,* 2016, **418**, 54. (f) M. Daraei, M. A. Zolfigol, F. Derakhshan-Panah, M. Shiri, H. G. Kruger, M. Mokhlesi, *J. Iran. Chem. Soc.*, 2015, **12**, 855. (g) M. Safaiee, M. A. Zolfigol, M. Tavasoli, M. Mokhlesi, *J. Iran. Chem. Soc.*, 2014, **11**, 1593; (h) D. Azarifar, S. M. Khatami, M. A. Zolfigol, R. Nejat-Yami, *J. Iran. Chem. Soc*, 2014, **11**, 1223.

[37] (a) M. A. Zolfigol, M. Yarie, *RSC Adv*., 2015, **5**, 103617.,(b) M. A. Zolfigol, M. Kiafar, M. Yarie, A. Taherpour, M . Saeidirad, *RSC Adv*. 2016, **6**, 50100.

[38] (a) M. A. Zolfigol, S. Baghery, A. R. Moosavi-Zare, S. M. Vahdat, H. Alinezhad, M. Norouzi, *RSC. Adv*., 2014, **4**, 57662., (b) M. A. Zolfigol, F. Afsharnaderee, S. Baghery, S. Salehzadeh, F. Maleki, *RSC Adv.* 2015**, 5**, 75555.

[39] A. Khazaei, A. R. Moosavi-Zare, H. Afshar-Hezarkhania and V. Khakyzadeh, *RSC Adv*., 2014, **4**, 32142.

[40] M. Nasr-Esfahani, D. Elhamifar, T. Amadeh, and B. Karimi, *RSC Adv*., 2015, **5**, 13087.

[41] O. Goli-Jolodar, F. Shirini and M. Seddighi, *RSC Adv*., 2016, *6*, 26026.

[42] C. X. Yu, D. Q. Shi, Q. Y. Zhuang and S. J. Tu, Chin. *J. Org. Chem*., 2006, **26**, 263.

[43] A. Davoodnia, M. Khashi, N. Tavakoli-Hoseini, *Chinese J. Catal.*, 2013, **34**, 1173.

[44] A. Heydari, S. Khaksar , M. Tajbakhsh, H. R. Bijanzadeh, *J. Fluorine Chem*., 2009, **130**, 609.

[45] A. Ghorbani-Choghamarani and G. Azadi, *RSC Adv.*, 2015, **5**, 9752.

[46] M. Nasr-Esfahani, D. Elhamifar, T. Amadeha and B. Karimi, *RSC Adv*., 2015, **5**, 13087.

[47] Z. Zarnegar, J. Safari and Z. M. Kafroudi, *New J. Chem*., 2015, **39**, 1445.

[48] M. Kidwai, R. Chauhan, D. Bhatnagar, A. K. Singh, B. Mishra and S. Dey, *Monatsh. Chem*., 2012, **143**, 1675.

[49] E. Mosaddegh and A. Hassankhani, *Arabian J. Chem*., 2012, **5**, 315.

[50] A. Khazaei, A. R. Moosavi-Zare, H. Afshar-Hezarkhania and V. Khakyzadeh, *RSC Adv*., 2014, **4**, 32142.

[51] M. B. Gawande, V. D. B. Bonif´acio, R. S. Varma, I. D. Nogueira, N. Bundaleski, C. A. A. Ghumman, O. M. N. D. Teodorod and P. S. Branco, *Green Chem.*, 2013, **15**, 1226.
[52] M. Hong, C. Cai and W. B. Yi, *J. Fluorine Chem*., 2010, **131**, 111.
[53] S. Qu, H. Yang, D. Ren, S. Kan, G. Zou, D. Li and M. Li, *J. Colloid Interface Sci*., 1999, **215**, 190.